Water Splitting

DOI: 10.1002/anie.201003110

Light-Induced Water Splitting with Hematite: Improved Nanostructure and Iridium Oxide Catalysis**

S. David Tilley, Maurin Cornuz, Kevin Sivula, and Michael Grätzel**

Photoelectrochemical (PEC) water splitting offers an elegant solution to the problem of collecting and storing energy on a global scale.[1] In a manner analogous to photosynthesis, solar energy is captured and stored in the form of chemical bonds to yield solar fuels, which can be used anytime energy is needed.[2]

Hematite has emerged as a strong candidate in the photoassisted water oxidation reaction because it is stable in water, prepared from cheap and abundant elements, and possesses a band gap that permits the absorption of visible light ($E_g = 2.1$ eV).[3] These favorable characteristics are balanced against the short lifetime of the excited-state carrier (10^{-12} s), small polaron-type charge transport, poor oxygen evolution reaction (OER) kinetics, and improper band positions for unassisted water splitting.[4] As such, much effort has been focused on studying and improving the performance of hematite photoanodes, however, the best performing hematite photoanodes are far from optimized as compared to materials such as TiO_2 and WO_3.[5]

Figure 1 shows the J-V curve of an ideal hematite photoanode (under AM 1.5 G 100 mW cm^{-2} light) and that of the former state-of-the-art hematite photoanode.[6] For the ideal case, the onset potential is just anodic (to the right) of the flat-band potential and the plateau current reaches 12.6 mA cm^{-2}, which corresponds to an incident photon to current efficiency (IPCE) of unity. In practice, the efficiency is limited by reflection and recombination losses. In addition, as the conduction band of hematite is lower than the water reduction potential, a bias must be applied, a bias that will ideally be generated by a photovoltaic (PV) device in tandem with a semitransparent hematite photoanode.[7] With the appropriate tandem PV setup, the maximum theoretical solar-to-hydrogen (STH) efficiency for a hematite photoanode is 15%.[8]

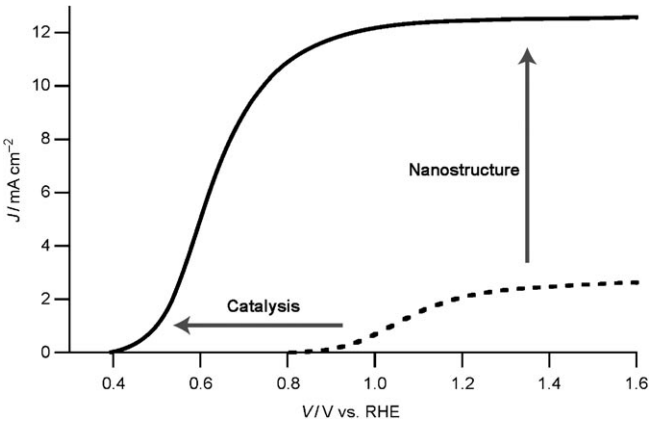

Figure 1. Idealized performance of the hematite photoanode (solid trace) compared with the former state-of-the-art hematite photoanode (dashed trace) under AM 1.5 G 100 mW cm^{-2} simulated sunlight.[6] The arrows indicate the parameters that need to be addressed to improve the anode.

The two most important metrics for the photocurrent curve are the plateau current and the onset potential.[9] The value of the plateau current gives an idea as to how many photogenerated holes are reaching the semiconductor/liquid junction (SCLJ). This assumes that at such high potentials all of the photogenerated holes react with water as opposed to recombining. The small polaron charge transport in hematite[10] requires high levels of doping to produce a material that is suitably conductive for water splitting. Unfortunately, high doping also results in a relatively thin space-charge layer, such that the majority of the photons are absorbed far from the space-charge field, which attracts the photogenerated holes to the SCLJ. Therefore, reducing the feature size of the semiconductor by nanostructuring has been utilized as a method to effectively increase the relative volume of the space-charge layer with respect to that of the bulk, thereby reducing recombination and increasing the plateau current.

In the state-of-the-art hematite photoanode shown in Figure 1, the onset potential of +0.9 V is substantially anodic of the flat-band potential (+0.4 V).[11] This large overpotential is thought to be caused mainly from the slow kinetics for water oxidation[4] that results in hole accumulation at the surface, and then subsequent surface recombination occurs until sufficiently positive potentials are achieved for appreciable charge transfer across the interface. The modification of the surface of the hematite electrode with a water oxidation catalyst that has less of a kinetic barrier for interfacial charge-

[*] Dr. S. D. Tilley, M. Cornuz, Dr. K. Sivula, Prof. Dr. M. Grätzel
Institut des Sciences et Ingénierie Chimiques
Ecole Polytechnique Fédérale de Lausanne
1015 Lausanne (Switzerland)
Fax: (+41) 21-693-4111
E-mail: kevin.sivula@epfl.ch
michael.graetzel@epfl.ch
Homepage: http://isic.epfl.ch/lpi

[**] We thank the Swiss Federal Office of Energy (Project number 102326, PECHouse) for financial support, F. Le Formal for scanning electron microscopy images, and E. Thimsen for helpful discussions. Dr. S. D. Tilley gratefully acknowledges the National Science Foundation (U.S.A.) for a postdoctoral fellowship (Award No. OISE-0853127).

Supporting information for this article is available on the WWW under http://dx.doi.org/10.1002/anie.201003110.

transfer would lower the amount of overpotential required and shift the curve to the left as shown in Figure 1.

To realize the full potential of hematite, a strategy that improves both the nanostructure, as well as the kinetics of the water oxidation reaction at the SCLJ is needed. Herein, we demonstrate significant improvement in the nanostructure of hematite, which results in a dramatic increase in the plateau current, as well as a substantial shift in the onset potential by modification of the surface with IrO_2 nanoparticles; this result has led us to achieve unprecedented water splitting photocurrents of over 3 mA cm^{-2} at +1.23 V versus the reversible hydrogen electrode (RHE) under AM1.5G 100 mW cm^{-2} simulated sunlight conditions. These photocurrents are unmatched by any other oxide-based photoanode operating under standard solar conditions.

Although many methods for controlling the morphology of hematite have been reported, it is rare to find reports of purposefully nanostructured hematite that performs well in a water splitting photoanode; factors such as doping, crystallinity, and substrate adhesion must be properly addressed. Our previously reported method using atmospheric pressure chemical vapor deposition took advantage of the high reactivity of an iron source, [$Fe(CO)_5$], which thermally decomposed to form nanoparticles that were entrained in the carrier gas.[6] These particles, along with the unreacted precursor, are deposited upon the substrate to create a cauliflower-type morphology. For similar particle-assisted deposition methods the critical factor in controlling the morphological and electronic properties of the films is the ratio of particles to unreacted precursor in the carrier gas stream.[12] Altering this parameter can be accomplished by changing the velocity of the gas stream, essentially changing the residence time of the gasses in the region of particle formation. However, changing the carrier-gas flow rate in turn affects the substrate temperature and other variables. We investigated the effects of changing the carrier-gas flow rate by setting the volumetric flow rate of air to 6 L min^{-1} (compared to the 2 L min^{-1} in reference [6]) and keeping the same concentration of the iron precursor. The heater temperature and the dopant concentration were then reoptimized. Electrodes prepared using the newly optimized deposition conditions[13] gave a higher photocurrent plateau (see below) compared to our previous results. Although the morphology of the thin films did not change drastically, the films with the highest photocurrents were those that were approximately 700 nm thick and prepared at 6 L min^{-1}; compared to the 400 nm thick film prepared under the optimized conditions at 2 L min^{-1} (Figure 2). As our previous work showed, electron transport in films prepared at 2 L min^{-1} became a limitation when the thickness was increased past 600 nm;[11] however, the optimum thickness (700 nm) for the 6 L min^{-1} case indicates the superior electron-transport properties of these electrodes. This could be a result of a smaller particle/precursor ratio afforded by the shorter gas residence time, which results in better adhesion between the particles as they attach to the growing film. Ongoing investigations are underway to fully understand the effect the residence time has on the optimum film performance.

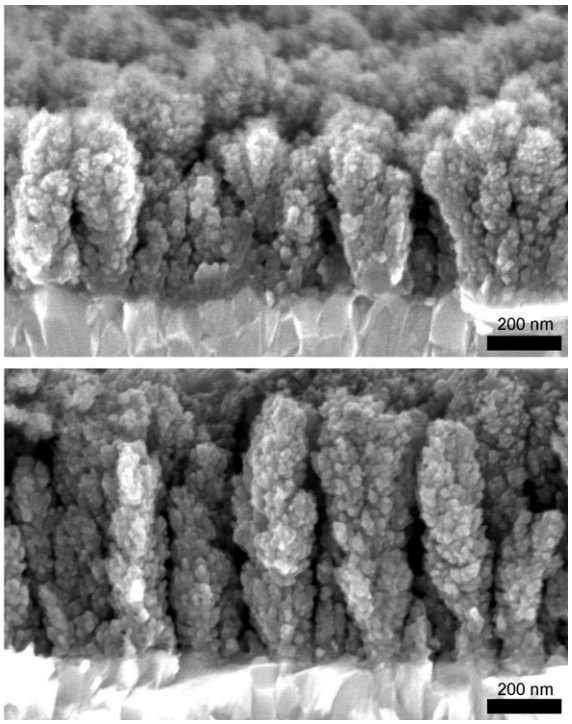

Figure 2. Scanning electron micrographs of the cross-section of the optimized Fe_2O_3 photoanodes prepared on F:SnO_2 substrates with carrier-gas flow rates of 2 L min^{-1} (a) and 6 L min^{-1} (b).

Although our work enhancing the nanostructure of the Fe_2O_3 afforded increased plateau photocurrents, the onset potential was unaffected. We next sought to improve the OER catalysis. Early investigations into catalysis on hematite photoanodes revealed that simply rinsing with a cobalt(II) nitrate solution yielded a 90 mV cathodic shift in the photocurrent curve and increased the plateau current by about 0.1 mA cm^{-2}.[6,14] The increase in the plateau current shows that even at very high potentials there is some degree of surface recombination that is at least partially ameliorated by the cobalt treatment. More recent work has demonstrated that a cobalt phosphate amorphous catalyst deposited onto the hematite surface shows a catalytic effect with similar results.[15] A photodeposition technique for a cobalt phosphate catalyst has also been demonstrated on ZnO electrodes.[16]

In terms of overpotential, iridium oxide (IrO_2) is the best water oxidation catalyst.[17] Small nanoparticles (ca. 2 nm diameter) deposited onto a glassy carbon electrode achieve quantitative Faradaic efficiency of water oxidation at overpotentials as low as 0.25 V (0.5 mA cm^{-2}).[18] For comparison, the cobalt phosphate catalyst, prepared from commonly available components, requires an overpotential of 0.40 V to achieve 0.5 mA cm^{-2}.[19] Thus, in an effort to achieve the lowest possible photocurrent onset potential and to also better understand the kinetic limitations of our photoanodes, we attempted to modify the surface of the hematite with IrO_2 nanoparticles.

IrO_2 nanoparticles (ca. 2 nm diameter) were deposited by electrophoresis onto the hematite photoanode,[13] and we

observed a dramatic shift in the onset potential from +1.0 V to +0.8 V versus RHE and an increase in the plateau photocurrent from 3.45 mA to 3.75 mA (Figure 3). This deposition method was found to be superior to methods such as soaking.[20] X-ray photoelectron spectroscopy (XPS)

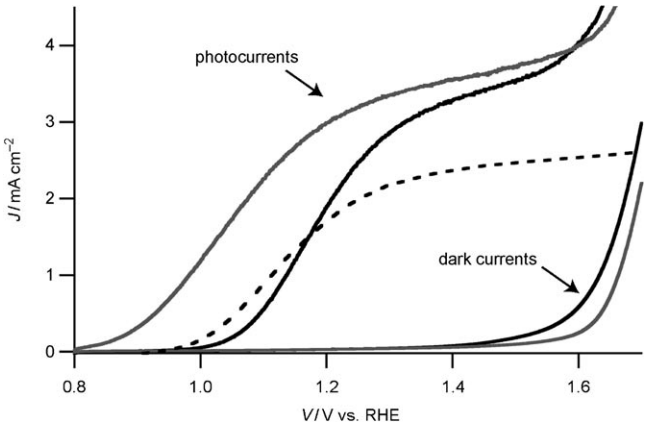

Figure 3. Performance of the unmodified hematite photoanode (solid black trace), and the same anode that was functionalized with IrO_2 nanoparticles (solid gray trace). Conditions: 1 M NaOH solution (pH 13.6), 10 mV s^{-1} scan rate, uncorrected for Ohmic losses. The corresponding dark currents are also shown. The dashed trace is the photocurrent for the former state-of-the-art hematite photoanode.[6,14] Photocurrents correspond to AM 1.5 G 100 mW cm^{-2} simulated sunlight.

revealed a surface concentration of iridium of 1.0 at. %. Along with the improvements in the nanostructure, this method has allowed us to achieve a new benchmark of greater than 3 mA cm^{-2} at +1.23 V versus RHE under AM 1.5 G 100 mW cm^{-2} simulated sunlight conditions. This current is the real photocurrent of the photoanode and is uncorrected for Ohmic resistance losses (ca. 60 Ohm).

To verify the value of the photocurrent at +1.23 V, we examined the incident photon to current efficiency (IPCE) as a function of photon wavelength. In accordance with previous work,[6] the value +1.23 V versus RHE was chosen as a metric to evaluate the performance of photoelectrodes because this potential corresponds to the reversible oxygen electrode. The IPCE was found to be over 50% at $\lambda_{max} = 320$ nm and to maintain a value of 21.4% closer to the band edge ($\lambda =$ 500 nm). These values are considerably higher than the previously reported data (46% and 14% at λ_{max} 320 nm and 500 nm, respectively). The proportionally larger increase at the longer wavelengths indicates that the improved nanostructure is better at harvesting longer wavelength photons and separating the electrons and holes to afford the water splitting reaction before charge carrier recombination takes place. Moreover, integrating the overlap of the IPCE data with the standard solar spectrum,[21] AM 1.5 G 100 mW cm^{-2}, gives a calculated value of the photocurrent of 3.01 mA cm^{-2} (Figure 4), confirming that the employed light source precisely simulated the AM 1.5 G solar emission in the absorption wavelength range of the hematite electrode; that is, the spectral mismatch was negligibly small.

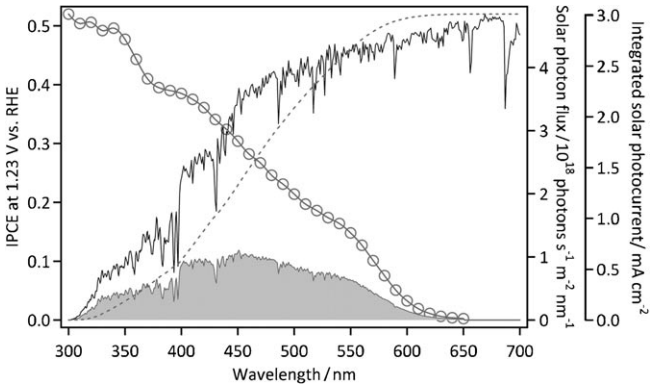

Figure 4. The incident photon conversion efficiency (IPCE) at an applied potential of +1.23 V versus RHE (circles, uncorrected for Ohmic losses) and the AM 1.5 G 100 mW cm^{-2} solar spectrum (dark trace) are multiplied together to give the number of photons stored in the form of hydrogen (shaded area). The dashed trace is the integrated photocurrent and reaches 3.01 mA cm^{-2}.

Notably, a slow decrease in the cathodic shift of the nanoparticle-modified hematite occurs upon successive scans, although the shift can be fully restored with the application of more IrO_2 nanoparticles. Additionally, chronoamperometry reveals a slight reduction in photocurrent over 200 seconds at +1.23 V versus RHE (Figure 5). These data indicate that the IrO_2 particles are not stably adhered to the hematite and detach from the surface. However, we are confident that the

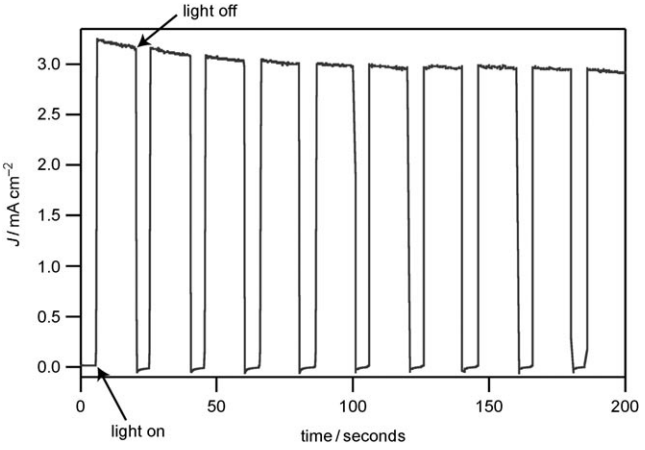

Figure 5. Chronoamperometry at an applied potential of +1.23 V versus RHE under light-chopping conditions (AM 1.5 G 100 mW cm^{-2}), uncorrected for Ohmic losses.

photocurrent is attributable solely to water oxidation because 1) there are no organic stabilizing ligands present for consumption, 2) strongly oxidizing conditions of the catalyst electrodeposition ensure that the iridium present in the nanoparticles begins in a highly oxidized state, and 3) these particles have been shown to achieve quantitative Faradaic efficiency at currents as low as 0.5 mA cm^{-2}. Interestingly, despite applying the best OER catalyst to the hematite and observing an unprecedented photocurrent under standard conditions, we still find the onset of the photocurrent to be at

a voltage that is 400 mV more positive than the flat-band potential, thereby suggesting that surface states having mid-band-gap energies facilitate the carrier recombination in hematite. Our previous work has identified a Raman-active amorphous fraction in these films that supports this observation.[11]

For the first time, a water splitting photocurrent of over 3 mA cm^{-2} has been achieved with hematite at an applied potential of +1.23 V versus RHE under AM1.5G 100 mW cm^{-2} simulated sunlight conditions. This significant advance in the performance of hematite indicates that the continued parallel optimization of both the nanostructure and the catalysis can ultimately realize the full potential of light-induced splitting of water into hydrogen and oxygen using iron oxide. Additional reduction of the overpotential required may come from applying recently reported surface treatments[22] or promising new catalysts for the oxygen evolution reaction.[23] We are currently investigating other techniques for customizing the nanostructure[24] and more robust methods for the attachment of the IrO_2 nanoparticles to the hematite.

Received: May 22, 2010
Published online: July 21, 2010

Keywords: hematite · iridium · photochemistry · supported catalysts · water splitting

[1] M. Grätzel, *Nature* **2001**, *414*, 338.
[2] a) R. van de Krol, Y. Q. Liang, J. Schoonman, *J. Mater. Chem.* **2008**, *18*, 2311; b) K. Rajeshwar, *J. Appl. Electrochem.* **2007**, *37*, 765.
[3] T. Lindgren, L. Vayssieres, H. Wang, S. E. Lindquist, *Chem. Phys. Nanostruct. Semicond.* **2003**, 83.
[4] a) M. P. Dare-Edwards, J. B. Goodenough, A. Hamnett, P. R. Trevellick, *J. Chem. Soc. Faraday Trans. 1* **1983**, *79*, 2027; b) J. B. Goodenough, *Prog. Solid State Chem.* **1971**, *5*, 145.
[5] a) M. Ni, M. K. H. Leung, D. Y. C. Leung, K. Sumathy, *Renewable Sustainable Energy Rev.* **2007**, *11*, 401; b) C. Santato, M. Ulmann, J. Augustynski, *J. Phys. Chem. B* **2001**, *105*, 936.
[6] A. Kay, I. Cesar, M. Grätzel, *J. Am. Chem. Soc.* **2006**, *128*, 15714. J-V curves were spectrally corrected; see note [14].
[7] J. Brillet, M. Cornuz, F. Le Formal, J. H. Yum, M. Grätzel, K. Sivula, *J. Mater. Res.* **2010**, *25*, 17.
[8] A. B. Murphy, P. R. F. Barnes, L. K. Randeniya, I. C. Plumb, I. E. Grey, M. D. Horne, J. A. Glasscock, *Int. J. Hydrogen Energy* **2006**, *31*, 1999.
[9] The plateau current can be defined as the highest value of photocurrent after subtraction of the dark current. The onset potential of the photocurrent (and dark current) can be determined by analysis of the derivative of the curve. See: F. Le Formal, M. Grätzel, K. Sivula, *Adv. Funct. Mater.* **2010**, *20*, 1099.
[10] A. J. Bosman, H. J. Vandaal, *Adv. Phys.* **1970**, *19*, 1.
[11] I. Cesar, K. Sivula, A. Kay, R. Zboril, M. Grätzel, *J. Phys. Chem. C* **2009**, *113*, 772.
[12] a) W. J. An, E. Thimsen, P. Biswas, *J. Phys. Chem. Lett.* **2010**, *1*, 249; b) E. Thimsen, N. Rastgar, P. Biswas, *J. Phys. Chem. C* **2008**, *112*, 4134; c) U. Backman, A. Auvinen, J. K. Jokiniemi, *Surf. Coat. Technol.* **2005**, *192*, 81.
[13] See the Supporting Information.
[14] Accounting for the spectral mismatch between the sun and the lamp is described in I. Cesar, PhD dissertation, Ecole Polytechnique Fédérale de Lausanne, Lausanne, **2007**.
[15] a) D. K. Zhong, J. Sun, H. Inumaru, D. R. Gamelin, *J. Am. Chem. Soc.* **2009**, *131*, 6086; b) D. K. Zhong, D. R. Gamelin, *J. Am. Chem. Soc.* **2010**, *132*, 4202.
[16] E. M. P. Steinmiller, K.-S. Choi, *Proc. Natl. Acad. Sci. USA* **2009**, *106*, 20633.
[17] a) J. Kiwi, M. Grätzel, *Angew. Chem.* **1978**, *90*, 900; *Angew. Chem. Int. Ed. Engl.* **1978**, *17*, 860; b) J. Kiwi, M. Grätzel, *Angew. Chem.* **1979**, *91*, 659; *Angew. Chem. Int. Ed. Engl.* **1979**, *18*, 624.
[18] a) T. Nakagawa, N. S. Bjorge, R. W. Murray, *J. Am. Chem. Soc.* **2009**, *131*, 15578; b) T. Nakagawa, C. A. Beasley, R. W. Murray, *J. Phys. Chem. C* **2009**, *113*, 12958.
[19] M. W. Kanan, D. G. Nocera, *Science* **2008**, *321*, 1072.
[20] R. Abe, M. Higashi, K. Domen, *J. Am. Chem. Soc.* **2010**, DOI: 10.1021/ja1016552.
[21] ASTM G-173-03, http://rredc.nrel.gov/solar/spectra/am1.5/.
[22] Y. S. Hu, A. Kleiman-Shwarsctein, G. D. Stucky, E. W. McFarland, *Chem. Commun.* **2009**, 2652.
[23] Q. S. Yin, J. M. Tan, C. Besson, Y. V. Geletii, D. G. Musaev, A. E. Kuznetsov, Z. Luo, K. I. Hardcastle, C. L. Hill, *Science* **2010**, *328*, 342.
[24] a) K. Sivula, F. Le Formal, M. Grätzel, *Chem. Mater.* **2009**, *21*, 2862; b) K. Sivula, R. Zboril, F. Le Formal, R. Robert, A. Weidenkaff, J. Tucek, J. Frydrych, M. Grätzel, *J. Am. Chem. Soc.* **2010**, *132*, 7436.

